

# Sign Determination of Coupling Constants in $\text{CF}_2\text{H}$ and $\text{CF}_3$ Derivatives of Silver(III)

Reint Eujen\* and Berthold Hoge

Anorganische Chemie, Fachbereich 9, Universität-GH, 42097 Wuppertal, Germany

The NMR spectra of the square-planar silver(III) anions  $[\text{Ag}(\text{CF}_3)_4]^-$  and  $[\text{Ag}(\text{CF}_2\text{H})_4]^-$  were investigated. The signs of  $^1J(^{109}\text{Ag}, ^{13}\text{C})$ ,  $^2J(^{109}\text{Ag}, ^{19}\text{F})$  and  $^2J(^{109}\text{Ag}, ^1\text{H})$  and those of the long-range couplings  $^4J(^{19}\text{F}, ^{19}\text{F})$ ,  $^3J(^{19}\text{F}, ^{13}\text{C})$ ,  $^3J(^{13}\text{C}, ^1\text{H})$  and  $^4J(^{19}\text{F}, ^1\text{H})$  were determined by analysis of higher order spin systems and from 2D heteronuclear correlations. All determined reduced coupling constants are positive with respect to  $^1J(^{13}\text{C}, ^1\text{H}) > 0$  or  $^1J(^{19}\text{F}, ^{13}\text{C}) < 0$ . Correlations between couplings for a variety of  $\text{CF}_3\text{Ag(III)}$  compounds suggest that no sign crossover occurs. © 1997 John Wiley & Sons, Ltd.

*Magn. Reson. Chem.* 35, 707–711 (1997) No. of Figures: 6 No. of Tables: 1 No. of References: 9

**Keywords:** NMR;  $^{109}\text{Ag}$  NMR,  $^{19}\text{F}$  NMR,  $^{13}\text{C}$  NMR; coupling constants; signs; fluoromethyl silver derivatives

Received 17 January 1997; revised 30 April 1997; accepted 12 May 1997

## INTRODUCTION

While the oxidation state +3 is unusual for silver, silver(III) can be stabilized by  $\text{CF}_3$  groups. The first such compound, the silver(I) argentate(III),  $\text{Ag}[\text{Ag}(\text{CF}_3)_4]$ , was described by Dukat and Naumann.<sup>1</sup> Dissolved in acetonitrile, it exhibits  $^{109}\text{Ag}$  resonances at +368 and +2233 ppm for the  $\text{Ag}^+$  and the  $[\text{Ag}(\text{CF}_3)_4]^-$  moieties, respectively, the intensity distribution of the multiplet of the latter signal being in accord with coupling to 12 equivalent fluorine nuclei. The square-planar coordination of the diamagnetic  $d^8$  silver(III) species has been established by x-ray crystallography.<sup>2</sup> Recently, we have succeeded in substituting up to three  $\text{CF}_3$  groups by ligands such as CN or  $\text{CH}_3$  groups.<sup>3</sup> Though the stability of these silver(III) derivatives diminishes as the number of  $\text{CF}_3$  groups attached to the silver atom decreases, low-temperature NMR studies often confirm unambiguously their composition and stereochemistry. Furthermore, we have shown<sup>4</sup> that  $\text{CF}_2\text{H}$ -substituted argentates(III) are also accessible. Thus,  $[\text{PNP}][\text{Ag}(\text{CF}_2\text{H})_4]$  has been isolated and characterized by x-ray crystallography.

The abundance of spin-1/2 nuclei [ $^{19}\text{F}$ ,  $^1\text{H}$ ,  $^{13}\text{C}$ ,  $^{109}\text{Ag}$  (48.2%) and  $^{107}\text{Ag}$  (51.8%)] makes these compounds suitable for NMR spectroscopic detection and characterization. Especially  $^{19}\text{F}$  NMR spectroscopy, with its pronounced response of chemical shifts to even minor changes in the chemical environment and characteristic short- and long-range couplings, is of high analytical importance. Despite their high abundance, the direct observation of the silver resonances is usually prevented by the low and negative magnetogyric ratios

of the silver nuclei and by long relaxation times.<sup>5</sup> In addition, the resonance frequency is at the low end of commercial broadband probes where the quality factor of the resonance circuit is low. These problems are widely compensated for by making use of the  $^2J(^{109}\text{Ag}, ^{19}\text{F})$  coupling, that is, by applying the DEPT or INEPT technique or by inverse detection. The DEPT pulse sequence with polarization transfer from the  $^{19}\text{F}$  nuclei can also be applied to enhance the sensitivity of  $^{13}\text{C}$  spectra. This technique simultaneously allows distinction and selection between  $^{13}\text{CF}_3$  and  $^{13}\text{CF}_2\text{H}$  resonances because of the pronounced differences in both  $^{19}\text{F}$  chemical shifts and  $^1J(^{13}\text{C}, ^{19}\text{F})$  couplings.

The high sensitivity of the NMR spectroscopic parameters such as  $^1J(^{109}\text{Ag}, ^{13}\text{C})$  and  $^2J(^{109}\text{Ag}, ^{19}\text{F})$  towards the chemical environment has been discussed previously in terms of competing participation of silver 5s and 4d orbitals in the bonding to the fluorinated methyl group.<sup>3</sup> Such a discussion of electronic influences is aided by the knowledge of the signs of the coupling constants. In this paper, we describe the determination of relative signs in fluorinated methylsilver compounds by means of two-dimensional spectroscopy and by simulation of higher order spin systems.

## RESULTS

The basic feature of the  $^{19}\text{F}$  resonance of a  $(\text{CF}_3)_n\text{Ag}$  unit consists of a pair of doublets with nearly equal intensities. The ratio of the couplings to the silver isotopes  $^{109}\text{Ag}$  and  $^{107}\text{Ag}$  amounts to 1.15. For  $n > 1$ , the couplings between the  $\text{CF}_3$  groups are considerable, especially between those groups which are *trans* to each other.

The  $^4J(^{19}\text{F}, ^{19}\text{F})$  coupling between chemically equivalent  $\text{CF}_3$  groups is discernible in the  $^{13}\text{C}$  satellites of the  $^{19}\text{F}$  resonance which are low-frequency shifted from the

\* Correspondence to: R. Eujen. E-mail: eujen@uni-wuppertal.de.  
Contract grant sponsor: Deutsche Forschungsgemeinschaft.  
Contract grant sponsor: Fonds der Chemischen Industrie.

main  $^{13}\text{C}$  system by 0.135 ppm and form the A part of an  $\text{A}_3\text{B}_{3(n-1)}\text{X}$  spin system. In  $\text{CF}_3$  derivatives of main group elements, these satellites may well be analyzed as a first-order system because the effective shift difference between the A and B resonances,  $^1J(^{13}\text{C}, ^{19}\text{F})/2 > 150$  Hz, is much larger than the  $^4J(^{19}\text{F}, ^{19}\text{F})$  coupling, provided that  $^3J(^{19}\text{F}, ^{13}\text{C})$  is also small. The number  $n$  of the  $\text{CF}_3$  groups attached to the central atom is thus readily derived from the multiplicity of the  $^{13}\text{C}$  satellites. Higher order effects are, however, clearly visible in high-quality  $^{13}\text{C}$  spectra of these compounds, and they allow the determination of the signs of both  $^4J(^{19}\text{F}, ^{19}\text{F})$  and  $^3J(^{19}\text{F}, ^{13}\text{C})$  couplings with respect to the negative  $^1J(^{19}\text{F}, ^{13}\text{C})$  constant. For example, positive signs for both long-range couplings could be derived for  $(\text{CF}_3)_3\text{As}^6$  or  $(\text{CF}_3)_2\text{Se}^7$  from the fine splitting of the quartet components and also by observation of extremely weak 'forbidden' lines between the main quartet components. When recorded as a  $^{13}\text{C}$  DEPT spectrum with polarization transfer from  $^{19}\text{F}$  and with an evolution time of  $0.5/^1J(\text{CF})$ s, these latter lines are so strongly phase shifted that they appear with negative intensity and are thus readily detected in low-noise spectra.

The situation is different for *trans*-( $\text{CF}_3$ ) $_2\text{Ag(III)}$  units. Higher order effects caused by large  $^4J(^{19}\text{F}, ^{19}\text{F})$  and  $^3J(^{19}\text{F}, ^{13}\text{C})$  couplings dominate the spectra, which are additionally complicated by the overlapping couplings to the  $^{109}\text{Ag}$  and  $^{107}\text{Ag}$  spins. The determination of the coupling constants thus requires a combined computer analysis of the  $^{13}\text{C}$  spectra and the  $^{13}\text{C}$  satellites of the

$^{19}\text{F}$  signals. The  $^{13}\text{C}$  spectrum of the anion  $[\text{Ag}(\text{CF}_3)_4]^-$  is shown in Fig. 1 along with its simulation. It is an example of an extremely complex  $\text{XA}_3\text{B}_3\text{C}_6\text{M}$  spin system where X is  $^{13}\text{C}$ , A, B and C refer to  $^{19}\text{F}$  either directly attached, *trans* or *cis* to  $^{13}\text{C}$ , respectively, and M is either  $^{109}\text{Ag}$  or  $^{107}\text{Ag}$ . The extreme line density of this spectrum does not allow a separation of lines attributable to the  $^{109}\text{Ag}$  and  $^{107}\text{Ag}$  sub-spectra. While  $^2J(^{109}\text{Ag}, ^{19}\text{F})$  and  $^1J(^{109}\text{Ag}, ^{13}\text{C})$  are readily available from the  $^{19}\text{F}$  and the fluorine-decoupled  $^{13}\text{C}$  spectra, respectively, the couplings across the silver atom have to be determined by an interactive fit to the basic spectral contour. The final parameters listed in Table 1 were obtained by a simultaneous lineshape analysis of the  $^{13}\text{C}$  spectrum and the  $^{13}\text{C}$  satellite system of the  $^{19}\text{F}$  resonance under consideration of both silver isotopes.

In general, all  $(\text{CF}_3)_n\text{Ag(III)}$  ( $n > 1$ ) systems studied so far are well simulated using positive signs of both  $^4J(^{19}\text{F}, ^{19}\text{F})$  and  $^3J(^{19}\text{F}, ^{13}\text{C})$  couplings with respect to the negative value of  $^1J(^{19}\text{F}, ^{13}\text{C})$ , regardless of whether *trans* or *cis* configurations are involved. The two correlations displayed in Fig. 2 indicate that these signs are not likely to switch. These correlations interconnect the couplings  $^1J(^{19}\text{F}, ^{13}\text{C})$ ,  $^3J(^{19}\text{F}, ^{13}\text{C})$  and  $^4J(^{19}\text{F}, ^{19}\text{F})$  of *trans*-( $\text{CF}_3$ ) $_2\text{Ag(III)}$  units in a variety of  $[\text{Ag}(\text{CF}_3)_2\text{R}_2]^-$  and  $[\text{Ag}(\text{CF}_3)_3\text{R}]^-$  species where R is  $\text{CF}_3$ ,  $\text{CN}$ ,  $\text{C}\equiv\text{CC}_6\text{H}_{11}$ , Cl, Br, I or a neutral donor molecule.<sup>3</sup> The smallest absolute values are found for the compounds containing covalently bonded methyl groups whereas the other end of the scale is formed by the

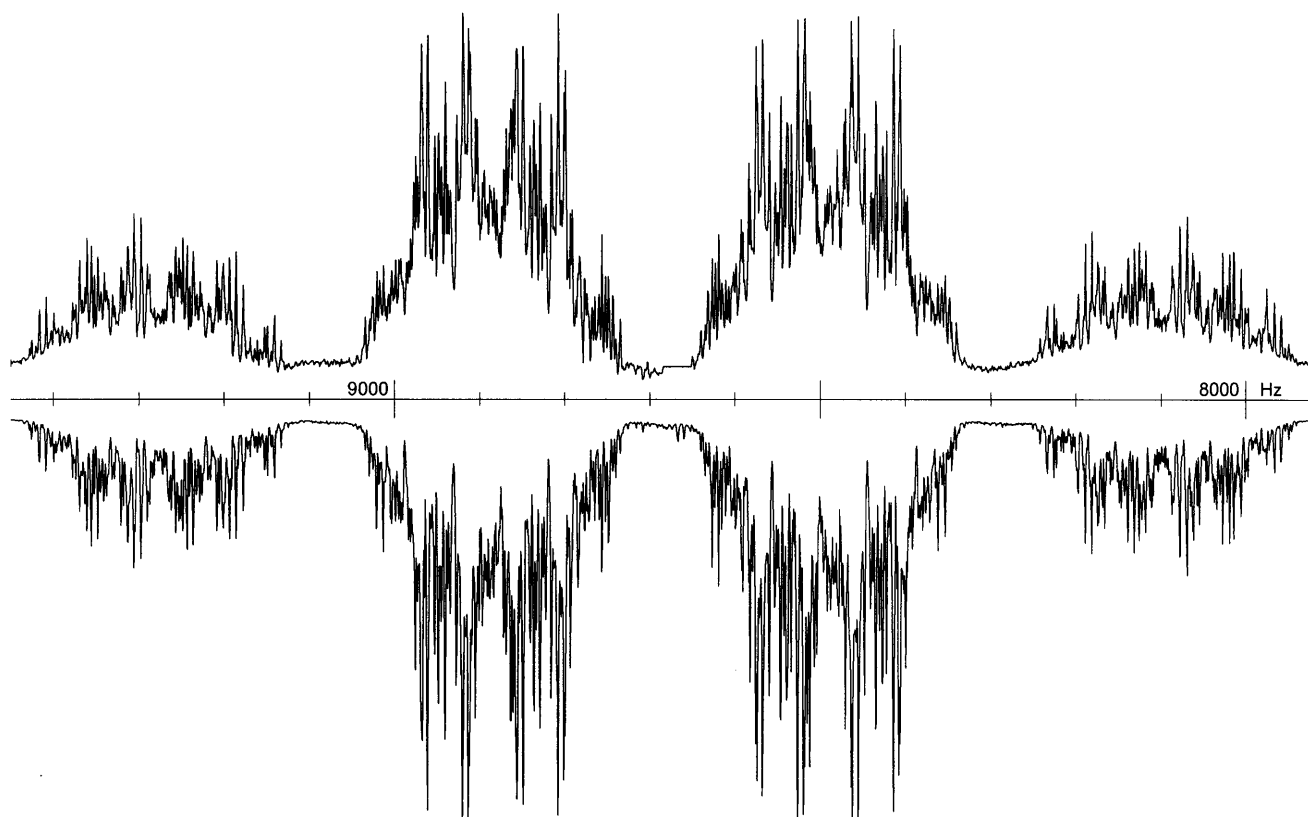


**Figure 1.** Experimental (up) and simulated (down) 62.9 MHz  $^{13}\text{C}$  spectra of the  $[\text{Ag}(\text{CF}_3)_4]^-$  anion. The experimental spectrum was recorded with polarization transfer from  $^{19}\text{F}$  (DEPT pulse sequence, variable pulse angle  $45^\circ$ , relaxation delay 2 s, transfer time  $\Delta$  1.25 ms, 8K data points, spectral width 1818 Hz, 28 000 scans).

**Table 1.** Chemical shifts and coupling constants of the complex anions  $[\text{Ag}(\text{CF}_2\text{H})_4]^-$  and  $[\text{Ag}(\text{CF}_3)_4]^-$  <sup>a</sup>

Parameter	$[\text{Ag}(\text{CF}_2\text{H})_4]^-$ <sup>b</sup>	$[\text{Ag}(\text{CF}_3)_4]^-$ <sup>c</sup>
$\delta^{109}\text{Ag}$	+2042	+2233
$\delta^{19}\text{F}$	-111.2	-32.7
$\delta^{13}\text{C}$	+140.1	+139.0
$\delta^1\text{H}$	+6.4	—
$^1J(^{109}\text{Ag}, ^{13}\text{C})$	-88.5	-120.0
$^2J(^{109}\text{Ag}, ^{19}\text{F})$	-24.4	-40.7
$^2J(^{109}\text{Ag}, ^1\text{H})$	-1.8	—
$^1J(^{19}\text{F}, ^{13}\text{C})$	-304.5	-393.1
$^3J(^{19}\text{F}, ^{13}\text{C})_{\text{trans}}$	+23.6	+45.8
$^3J(^{19}\text{F}, ^{13}\text{C})_{\text{cis}}$	(+ )9.4	+8.2
$^4J(^{19}\text{F}, ^{19}\text{F})_{\text{trans}}$	+7.3	+12.8
$^4J(^{19}\text{F}, ^{19}\text{F})_{\text{cis}}$	$\sim (\pm) 1.5$	+6.2
$^1J(^{13}\text{C}, ^1\text{H})$	+171.3	—
$^3J(^{13}\text{C}, ^1\text{H})_{\text{trans}}$	+8.6	—
$^3J(^{13}\text{C}, ^1\text{H})_{\text{cis}}$	( $\pm$ )2.9	—
$^2J(^{19}\text{F}, ^1\text{H})$	+46.6	—
$^4J(^{19}\text{F}, ^1\text{H})_{\text{trans}}$	+1.8	—

<sup>a</sup> Chemical shifts in ppm with reference to 1 M  $\text{AgNO}_3$  in  $\text{D}_2\text{O}$  ( $^{109}\text{Ag}$ ), TMS ( $^1\text{H}$ ,  $^{13}\text{C}$ ) and  $\text{CFCl}_3$  ( $^{19}\text{F}$ ); coupling constants in Hz.

<sup>b</sup> As  $[\text{PNP}][\text{Ag}(\text{CF}_2\text{H})_4]$  in  $\text{CDCl}_3$ , recorded at 298 K.

<sup>c</sup> As  $[\text{Ag}][\text{Ag}(\text{CF}_3)_4]$  in  $\text{CD}_3\text{CN}$ , recorded at 298 K.

dihalide  $[\text{trans-Ag}(\text{CF}_3)_2\text{Br}_2]^-$  with its more polar Ag—Br bonds. The neutral solvent complexes  $[\text{Ag}(\text{CF}_3)_3(\text{N}\equiv\text{CCH}_3)]$  and  $[\text{Ag}(\text{CF}_3)_3(\text{DMF})]$  exhibit the largest couplings within the series of  $(\text{CF}_3)_3\text{Ag}$

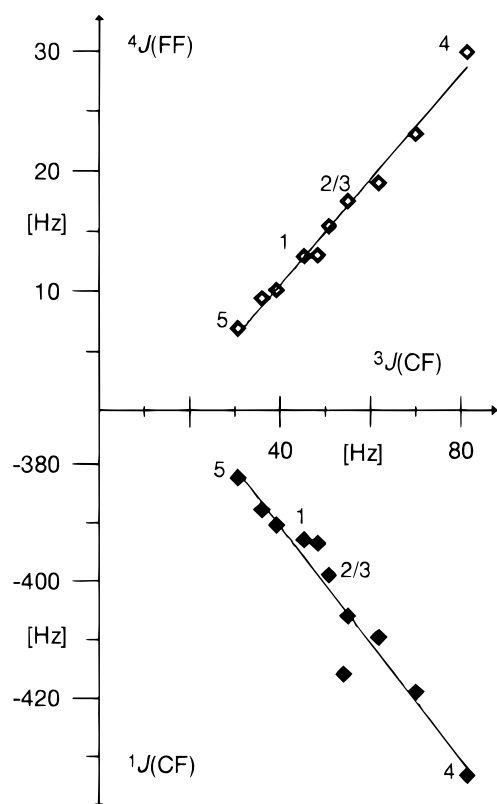


**Figure 2.** Correlation of  $^3J(^{19}\text{F}, ^{13}\text{C})$  vs.  $^4J(^{19}\text{F}, ^{19}\text{F})$  (top) and vs.  $^1J(^{19}\text{F}, ^{13}\text{C})$  (bottom) of *trans*-oriented  $\text{CF}_3$  groups in  $(\text{CF}_3)_n\text{Ag}(\text{III})$  derivatives. Characteristic points: 1,  $[\text{Ag}(\text{CF}_3)_4]^-$ ; 2,  $[\text{Ag}(\text{CF}_3)_3\text{Cl}]^-$ ; 3,  $[\text{Ag}(\text{CF}_3)_3(\text{DMF})]$ ; 4,  $[\text{Ag}(\text{CF}_3)_2\text{Br}_2]^-$ ; 5,  $[\text{Ag}(\text{CF}_3)_2(\text{CH}_3)_2]^-$ . Values were taken from Ref. 3.

derivatives. The cationic species  $[\text{Ag}(\text{CF}_3)_2(\text{DMF})_2]^+$  deviates from the  $^1J(^{19}\text{F}, ^{13}\text{C})/^3J(^{19}\text{F}, ^{13}\text{C})$  correlation.

The couplings to silver,  $^2J(^{109}\text{Ag}, ^{19}\text{F})$  and  $^1J(^{109}\text{Ag}, ^{13}\text{C})$ , are well correlated, as demonstrated by Fig. 3, which summarizes all currently known data. In those cases investigated by  $^{13}\text{C}/^{19}\text{F}$  2D heterocorrelation spectra, these constants have the same (negative) sign. The quality of the correlation indicates that this is valid for all silver(III) species prepared so far, although the electronic influence of the ligands leads to substantial variations in the magnitude of the coupling constants. The smallest absolute values are found for those complexes which contain more polar ligands such as the *trans*-dihaloargentates(III)  $[\text{Ag}(\text{CF}_3)_2\text{X}_2]^-$ , while the corresponding methyl derivative with its less polar Ag—CH<sub>3</sub> bond is at the other end of the scale. This dependence on the character of the ligands is opposite to that observed for main group elements and is related to the energetic sequence of the orbitals mainly constituting the metal—CF<sub>3</sub> bonds.<sup>3</sup> In transition metal compounds, the *ds* hybrid orbital with higher *s* character is used for forming the more polar bonds. In the case of main group elements, the *s* character is higher in those *sp* hybrids which are directed towards the more covalently bonded substituents.

Owing to the presence of protons, even more spectral information is available for  $\text{CF}_2\text{H}$ -substituted argentates(III). *trans*- $\text{Ag}(\text{CF}_2\text{H})_2$  units yield characteristic  $[\text{A}(\text{X})_2]_2\text{M}$  signal patterns ( $\text{A} = ^1\text{H}$ ;  $\text{X} = ^{19}\text{F}$ ;  $\text{M} = ^{109}\text{Ag}$  or  $^{107}\text{Ag}$ ) while fine structure in the corresponding signals of *cis* units is not resolved owing to the much smaller couplings. The analysis of  $^{19}\text{F}$  decoupled  $^{13}\text{C}$  spectra distinguishes between *cis* and *trans* isomers since  $^3J(^{13}\text{C}, ^1\text{H})_{\text{trans}}$  is distinctly larger than  $^3J(^{13}\text{C}, ^1\text{H})_{\text{cis}}$ .

Although high-quality spectra are available for the  $[\text{Ag}(\text{CF}_2\text{H})_4]^-$  anion, its spin system is too complex to be analyzed without constraints. Hence couplings between protons were neglected and the  $^4J(^{19}\text{F}, ^{19}\text{F})$  constants of the *cis*- $[\text{A}(\text{X})_2]_2$  sub-system were averaged. For example, the  $^1\text{H}$  decoupled  $^{13}\text{C}$  spectrum of this ion is approximated as an  $\text{X}[\text{A}]_2[\text{B}]_2\text{C}_4\text{M}$  system ( $\text{X} = ^{13}\text{C}$ ;  $\text{A}, \text{B}, \text{C} = ^{19}\text{F}$ ,  $\text{M} = ^{107}\text{Ag}$  or  $^{109}\text{Ag}$ ), which

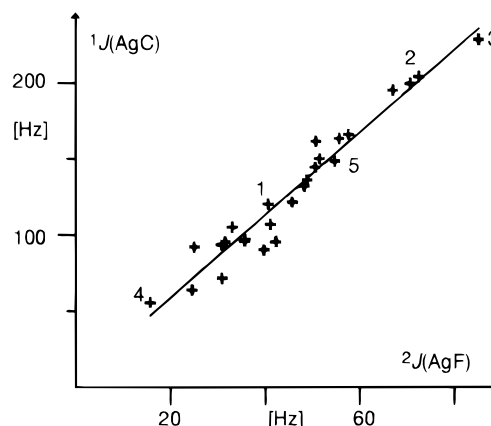


**Figure 3.** Correlation of  $^2J(^{109}\text{Ag}, ^{19}\text{F})$  vs.  $^1J(^{109}\text{Ag}, ^{13}\text{C})$  in  $(\text{CF}_3)_n\text{Ag}(\text{III})$  derivatives. Characteristic points: 1,  $[\text{Ag}(\text{CF}_3)_4]^-$ ; 2,  $[\text{Ag}(\text{CF}_3)_3\text{Cl}]^-$  (*cis*); 3,  $[\text{Ag}(\text{CF}_3)_3(\text{DMF})]$  (*cis*); 4,  $[\text{Ag}(\text{CF}_3)_2\text{Br}_2]^-$ ; 5,  $[\text{Ag}(\text{CF}_3)_2(\text{CH}_3)_2]^-$ . Values were taken from Refs 3 and 4.

gives excellent agreement between experimental and calculated spectra (Table 1). Information on relative signs is obtained from a series of 2D spectra which are displayed in Figs 4–6.

Figure 4 shows the  $^{109}\text{Ag}/^{19}\text{F}$  heterocorrelation spectrum of the  $[\text{Ag}(\text{CF}_2\text{H})_4]^-$  anion along with its  $^{19}\text{F}$  decoupled  $^{109}\text{Ag}$  spectrum as an  $f_2$  trace. The  $f_1$  projection reproduces the normal  $^{19}\text{F}$  spectrum and should not be mistaken for the  $f_1$  trace of the 2D spectrum. The latter basically consists of the silver decoupled HF doublet or, more precisely, the  $[\text{A}(\text{X})_2]_2$  spin system of the *trans*- $\text{CF}_2\text{H}$  groups. Line A correlates the HF doublet with the AgH quintet, and its positive slope shows that the reduced coupling constants  $^2K(^{19}\text{F}, ^1\text{H})$  and  $^2K(^{109}\text{Ag}, ^1\text{H})$  have the same sign. Since  $\gamma(^{109}\text{Ag})$  is

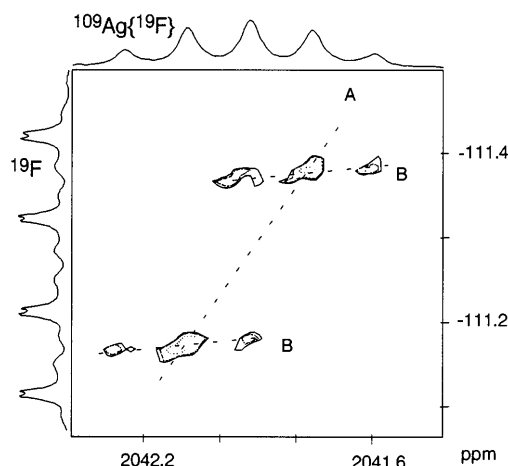


**Figure 4.** Contour plot of the  $^{109}\text{Ag}/^{19}\text{F}$  2D spectrum of the  $[\text{Ag}(\text{CF}_2\text{H})_4]^-$  anion. The  $f_2$  projection shows the quintet  $[^2J(^{109}\text{Ag}, ^1\text{H})]$  of the  $^{19}\text{F}$  decoupled 11.6 MHz  $^{109}\text{Ag}$  spectrum. The  $^{19}\text{F}$  spectrum with its basic doublet of doublet splitting  $[^2J(^{19}\text{F}, ^1\text{H})]$  and  $[^1J(^{109}\text{Ag}, ^{19}\text{F})]$  is displayed as an  $f_1$  projection. Spectral parameters: 64 data points and spectral width of 200 Hz in  $f_1$ ; 512 data points and spectral width of 74 Hz in  $f_2$ ; 16 scans; mixing delay  $\tau$  20.4 ms; refocusing delay  $\Delta$  6 ms; recycle time 5 s.

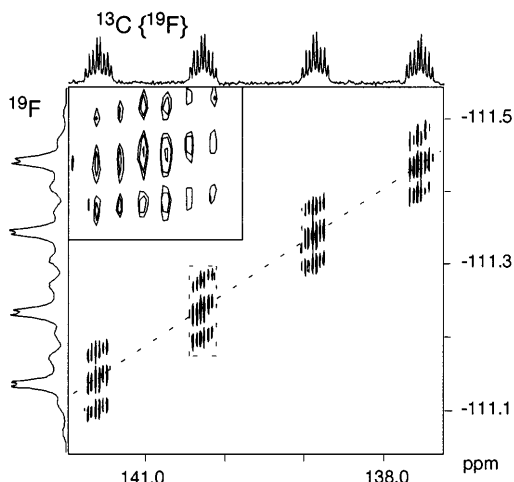


**Figure 5.** Contour plot of the  $^{13}\text{C}/^{19}\text{F}$  heterocorrelation spectrum of the  $[\text{Ag}(\text{CF}_2\text{H})_4]^-$  anion with the  $^{19}\text{F}$  decoupled  $^{13}\text{C}$  spectrum as an  $f_2$  (see text) and the  $^{19}\text{F}$  spectrum as an  $f_1$  projection, the scale of the latter being corrected for the  $^{13}\text{C}/^{12}\text{C}$  isotope shift. The inset shows an expansion of one multiplet component. Spectral parameters: 128 data points and spectral width of 500 Hz in  $f_1$ ; 2048 data points and spectral width of 512 Hz in  $f_2$ ; 64 scans; mixing delay  $\tau$  1.6 ms; refocusing delay  $\Delta$  0.8 ms; recycle time 4 s.

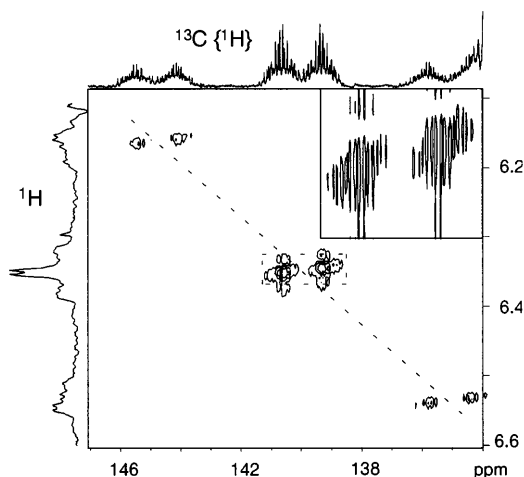


**Figure 6.** Contour plot of the  $^{13}\text{C}/^1\text{H}$  2D spectrum of the  $[\text{Ag}(\text{CF}_2\text{H})_4]^-$  anion with the  $^1\text{H}$  decoupled  $^{13}\text{C}$  spectrum as an  $f_2$  (see text) and the  $^1\text{H}$  spectrum as an  $f_1$  projection. The inset shows an expansion of the central cluster. Spectral parameters: 128 data points and spectral width 400 Hz in  $f_1$ ; 4096 data points and spectral width 1706 Hz in  $f_2$ ; 320 scans; mixing delay  $\tau$  2.9 ms; refocusing delay  $\Delta$  2.9 ms; recycle time 4 s.

negative, opposite signs are thus obtained for  $^2J(^{19}\text{F}, ^1\text{H})$  and  $^2J(^{109}\text{Ag}, ^1\text{H})$ . A closer inspection of the 2D spectrum reveals a small but significant positive tilt within the two basic clusters indicated by the lines B, which correlates  $^2K(^{109}\text{Ag}, ^1\text{H})$  with the long-range *trans* coupling  $^4K(^{19}\text{F}, ^1\text{H})_{\text{trans}}$ . Consequently, the signs of  $^4J(^{19}\text{F}, ^1\text{H})_{\text{trans}}$  and  $^2J(^{109}\text{Ag}, ^1\text{H})$  are also opposite; therefore, those of  $^4J(^{19}\text{F}, ^1\text{H})_{\text{trans}}$  and  $^2J(^{19}\text{F}, ^1\text{H})$  are identical. Both relative signs and absolute values of the latter couplings are independently verified by computer simulation of the respective  $^1\text{H}$  and  $^{19}\text{F}$  spectra of *trans*-( $\text{CF}_2\text{H}$ ) $_2\text{Ag}$  units.

The  $^{13}\text{C}/^{19}\text{F}$  2D spectrum of  $\text{Ag}(\text{CF}_2\text{H})_4^-$  is displayed in Fig. 5, again with the  $^{19}\text{F}$  spectrum as an  $f_1$  projection. The isotope shift  $\delta(^{12}\text{CF}_2\text{H}) - \delta(^{13}\text{CF}_2\text{H})$  of 0.101 ppm has been eliminated by re-referencing in order to simplify the presentation. The  $f_2$  projection contains the  $^{19}\text{F}$  decoupled  $^{13}\text{C}$  spectrum. Basically it is a doublet of doublet pattern where the larger  $^1J(^{13}\text{C}, ^1\text{H})$  coupling is approximately twice the value of  $^1J(^{109}\text{Ag}, ^{13}\text{C})$ . The fine structure appears simple because  $^3J(^{13}\text{C}, ^1\text{H})_{\text{trans}}$  amounts to  $3 \times ^3J(^{13}\text{C}, ^1\text{H})_{\text{cis}}$  and the  $^{109}\text{Ag}/^{107}\text{Ag}$  splitting is approximately twice the value of  $^3J(^{13}\text{C}, ^1\text{H})_{\text{cis}}$ . The main tilt given by the broken line confirms that the signs of  $^1J(^{13}\text{C}, ^1\text{H})$  and  $^2J(^{19}\text{F}, ^1\text{H})$  are equal. Inspection of the inset reveals a positive tilt within each cluster which correlates the long-range couplings  $^3J(^{13}\text{C}, ^1\text{H})_{\text{trans}}$  and  $^4J(^{19}\text{F}, ^1\text{H})_{\text{trans}}$ .

The relationship between the basic  $^{13}\text{CF}_2$  triplet structure ( $f_2$  projection) and the  $^1\text{H}$  spectrum shown in the  $f_1$  projection of the  $^{13}\text{C}/^1\text{H}$  shift correlation (Fig. 6) confirms that  $^1J(^{19}\text{F}, ^{13}\text{C})$  and  $^2J(^{19}\text{F}, ^1\text{H})$  have opposite signs (broken line). A basic triplet pattern for the  $\text{CF}_2\text{H}$  group is perceivable in the higher order  $^1\text{H}$  spectrum and the small AgH doublet splitting is clearly discernible in the central part. The inset in Fig. 6 contains a magnification of the central pattern which is split into two clusters by the AgC couplings. The positive tilt of these two clusters yields equal signs for  $^1J(^{109}\text{Ag}, ^{13}\text{C})$  and  $^2J(^{109}\text{Ag}, ^1\text{H})$ , which are consequent-

ly negative. Finally, the tilt within each cluster connects  $^3J(^{19}\text{F}, ^{13}\text{C})_{\text{trans}}$  and  $^4J(^{19}\text{F}, ^1\text{H})_{\text{trans}}$ , both being positive.

An attempt to relate the sign of the  $^1J(^{109}\text{Ag}, ^{13}\text{C})$  coupling in  $[\text{Ag}(\text{CF}_3)_4]^-$  to the negative  $^1J(^{19}\text{F}, ^{13}\text{C})$  coupling by observation of the  $^{13}\text{C}$  satellites in the  $^{109}\text{Ag}/^{19}\text{F}$  shift correlation gave evidence for but not a final proof of a negative value. However, selective  $^{19}\text{F}$  homodecoupling experiments on the  $\text{CF}_3$  doublets in argentates(III) which contain both  $\text{CF}_3$  and  $\text{CF}_2\text{H}$  groups<sup>4</sup> clearly demonstrate that the  $^2J(^{109}\text{Ag}, ^{19}\text{F})$  couplings in  $(\text{CF}_3)_2\text{Ag(III)}$  and  $(\text{CF}_2\text{H})\text{Ag(III)}$  units possess the same (negative) sign.

To summarize, the determination of the signs of coupling constants involving the  $^{109}\text{Ag}$  nucleus and of long-range couplings across silver in  $(\text{CF}_3)_n\text{Ag(III)}$  and  $(\text{CF}_2\text{H})_n\text{Ag(III)}$  units has been achieved by using 2D experiments and computer simulations of higher order 1D spectra. The relevant couplings to the two complex anions  $[\text{Ag}(\text{CF}_3)_4]^-$  and  $[\text{Ag}(\text{CF}_2\text{H})_4]^-$  are listed in Table 1. All couplings to silver(III) exhibit a negative sign, the respective reduced coupling constants being positive. The equal signs of  $^2J(^{109}\text{Ag}, ^1\text{H})$  and  $^2J(^{109}\text{Ag}, ^{19}\text{F})$  are in full accord with results obtained for  $\text{CF}_2\text{H}$  derivatives of Group 14 elements where the reduced coupling constants  $^2K(\text{M}, ^1\text{H})$  ( $\text{M} = ^{29}\text{Si}$ ,  $^{119}\text{Sn}$  or  $^{207}\text{Pb}$ ) are positive, in contrast to the negative signs usually found in  $(\text{CH}_3)\text{M}$  and  $(\text{CH}_2\text{F})\text{M}$  derivatives.<sup>7</sup> It may be predicted that the comparatively large  $^2J(^{109}\text{Ag}, ^1\text{H})$  constants found in  $\text{CH}_3\text{Ag(III)}$  compounds<sup>3</sup> have an opposite, that is, positive, sign.

## EXPERIMENTAL

NMR spectra were recorded with a Bruker ARX 400 instrument ( $^1\text{H}$  400.13 MHz;  $^{13}\text{C}$  100.63 MHz;  $^{19}\text{F}$  376.50 MHz) or a Bruker AC 250 ( $^1\text{H}$  250.13 MHz;  $^{19}\text{F}$  235.36 MHz;  $^{13}\text{C}$  62.90 MHz;  $^{109}\text{Ag}$  11.64 MHz). The latter spectrometer was equipped with a  $^{19}\text{F}$  decoupler

which used the pulse trains generated by the  $^1\text{H}$  decoupler. For this purpose, the  $(^1\text{H} + \text{O}_2)/3$  frequency, ca. 83.38 MHz, was mixed with 4.93 MHz from a second synthesizer. The lower side band was selected by a low-pass filter, tripled and amplified using a Bruker B-SV3 BX unit, the levels for high power pulses and CPD decoupling being set via the mismatch control. This arrangement allowed  $^{19}\text{F}$  broadband decoupling over a range of more than 20 kHz after tuning the decoupler coil to the fluorine frequency. If possible, polarization transfer from  $^{19}\text{F}$  by means of the DEPT pulse sequence was used to record the 1D spectra of less sensitive nuclei such as  $^{13}\text{C}$  and  $^{109}\text{Ag}$ . Two-dimensional spectra ( $^{13}\text{C}/^{19}\text{F}$ ,  $^{13}\text{C}/^1\text{H}$ ,  $^{109}\text{Ag}/^{19}\text{F}$ ) taken with the pulse sequence given by Bax and co-workers<sup>8</sup> were used for assignments and for determination of the relative signs of coupling constants. Relevant  $90^\circ$  pulse widths for the employed 10 mm probe were 40  $\mu\text{s}$  for  $^{109}\text{Ag}$  and 13.4  $\mu\text{s}$  for  $^{13}\text{C}$  spectra while the  $^{19}\text{F}$  decoupler used 19  $\mu\text{s}$  for high-power and 77  $\mu\text{s}$  for CPD pulses, the respective values for the  $^1\text{H}$  decoupler being 22 and 138  $\mu\text{s}$ . Variable-angle pulses of  $45^\circ$  and transfer delays  $\Delta$  of  $0.5/^1J(^{13}\text{C}, ^{19}\text{F})$  s were used for  $^{13}\text{C}$ - $^{19}\text{F}$  DEPT spectra and ca.  $25$ – $45^\circ$ , depending on the multiplicity, and  $0.5/^2J(^{109}\text{Ag}, ^{19}\text{F})$  s were applied for recording the  $^{109}\text{Ag}$  spectra, the recycle delays being 3–5 s. The delays in the 2D sequence were adapted correspondingly. Spectra were referenced to TMS ( $^1\text{H}$ ),  $\text{CDCl}_3$  at 77.0 ppm or  $\text{CD}_3\text{CN}$  at 1.3 ppm ( $^{13}\text{C}$ ), external  $\text{CFCl}_3$  ( $^{19}\text{F}$ ) and 1 M  $\text{AgNO}_3$  in  $\text{D}_2\text{O}$  ( $^{109}\text{Ag}$ ) ( $\Xi = 4.653\,561$  MHz). Computer simulations of higher order NMR spectra were carried out with the program gNMR.<sup>9</sup>

Samples were prepared following published procedures.<sup>1,3,4</sup>

## Acknowledgements

Financial support by the Deutsche Forschungsgemeinschaft and the Fonds der Chemischen Industrie is gratefully acknowledged.

## REFERENCES

1. W. Dukat and D. Naumann, *Rev. Chim. Min.* **23**, 589 (1986).
2. (a) U. Geiser, J. A. Schlueter, J. M. Williams, D. Naumann and T. Roy, *Acta Crystallogr., Sect. B* **51**, 789 (1995); (b) T. Roy, Dissertation, Universität Köln (1993).
3. R. Eujen, B. Hoge and D. J. Brauer, *Inorg. Chem.* **36**, 1464 (1997).
4. R. Eujen, B. Hoge and D. J. Brauer, *Inorg. Chem.* in press.
5. R. K. Harris and B. E. Mann, *NMR and the Periodic Table*. Academic Press, London (1978).
6. R. Eujen and B. Hoge, *J. Organomet. Chem.* **503**, C51 (1995).
7. R. Eujen, to be published.
8. (a) A. Bax and G. A. Morris, *J. Magn. Reson.* **42**, 501 (1981); (b) A. Bax, *J. Magn. Reson.* **53**, 517 (1983); (c) J. A. Wilde and P. H. Bolten, *J. Magn. Reson.* **59**, 343 (1984).
9. P. H. M. Budzelaar, *gNMR Version 3.65*. Cherrwell Scientific, Oxford (1996).